Available on CMS information server

CMS NOTE 2000/064

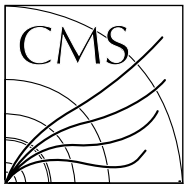

The Compact Muon Solenoid Experiment

CMS Note

Mailing address: CMS CERN, CH-1211 GENEVA 23, Switzerland

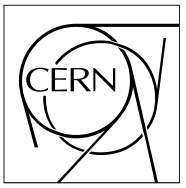

October 24, 2000

Thermal Regulation of the CMS Preshower Windows

P. Bloch[1], J. Rochez[2], P. Wertelaers[3], M. Zupan[3]

CERN, Geneva, Switzerland

1.ECAL Group, 2.IT-CO Group, 3.EP-TA2 Group

Abstract

A prototype Preshower (SE) ‘window’ has been used to test the viability of a thermal regulation scheme whose final purpose is to maintain the inside of the Preshower at a low temperature (-10 degrees C) whilst presenting an ambient (18 degrees C) temperature to neighbouring detectors. A simple control layout with coarse segmentation was found to be sufficient, foregoing the need for a complex multivariable controller.

The measurements are in agreement with simulation and confirm that a stabilization in time of the SE external faces within a few tenths of a degree can be achieved, as required by the Endcap ECAL.

1 Introduction

Due to the radiation damage of the silicon sensors, the CMS Preshower (SE) [1] detector must operate at a subzero temperature in its interior. It is required, however, that the surface of the detector remains at ambient temperature to avoid adverse thermal effects on neighbouring detectors as well as other unwanted effects such as condensation.

The Preshower detector is enclosed in a gas-tight cylindrical vessel. The flat faces of the vessel present two major surfaces towards the rest of the CMS detector. One faces the central Tracking Detector and the other faces the Endcap Electromagnetic Calorimeter (EE). These flat faces (so-called "windows") are 2.6 m outer diameter disks built from a sandwich of paraffin-filled aluminium honeycombs between aluminium skins. They act both as structural elements for the complete assembly and as a neutron moderator for the preshower. For mechanical reasons, the windows themselves are kept at room temperature and are thermally separated from the Preshower interior by an insulation foam. On the internal surface of each window a heating film is adhered. The heating film is a thin polyimide-encased layer of flat copper heating elements and it is used to regulate the temperature of the window. Between these windows lies the layered structure of the Preshower detector. These layers include cooling screens, lead absorbers, silicon detector planes with electronics (Fig. 1).

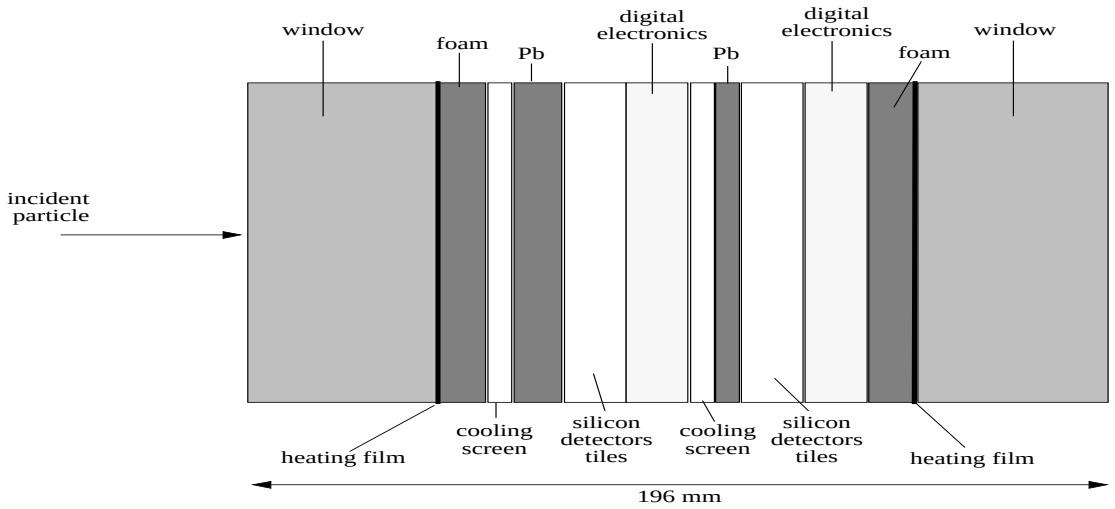

Figure 1: Schematic cross section of the Preshower detector (SE)

The energy response of the Endcap Electromagnetic Calorimeter is strongly temperature dependent. The temperature regulation of the Preshower window surface facing the calorimeter has therefore to be precise and stable to within 0.5°C . To achieve this performance, the power of the heating film is controlled with a feedback loop system.

In this note, we present both the design of the temperature control of the Preshower windows and the results of measurements done during July 2000 on a window prototype of reduced size but identical structure as the final product.

Section 2 presents the proposed layout of the heating film, the temperature regulation mechanism and the results of 3D finite element modelling showing the existence of a stable closed loop regime where external power attacks and disturbances of the internal Preshower temperature are efficiently rejected. The window prototype is described in section 3. The regulation system (hardware and software) used for the prototype is presented in section 4. In section 5 we report measurements of the frequency response of the window in open loop which can be directly compared to the predictions of section 2. Long term stability and disturbance rejection measurements in the closed loop regime are finally presented in section 6.

2 Design of the temperature control of the Preshower windows

2.1 Description of the Preshower windows

The cross section of a Preshower window is shown in Fig. 2 . It consists of a 38 mm thick aluminium honeycomb structure glued between two 1mm thick aluminium skins and filled with paraffin to act as neutron moderator. The paraffin filling efficiency (estimated from the weight of the prototype panel before and after filling) is 82%. On the internal face of the window (B on Fig. 2) is glued a thin heating film made of a flat copper conductor encased in kapton layers. The window is thermally insulated from the cold Preshower interior by a 10 mm thick foam.

The goal of the design and of the temperature regulation is to obtain an accurate, constant in time and spatially uniform temperature on the exterior face (C on Fig. 2).

2.2 Spatial property of the window in a simplified model

In a first approach[a)], we consider a very simplified pseudo 1D model where the window has an infinite extension. The assumed window's through-thickness properties are the following:

- foam : thickness s_1 = 10 mm, conductibility λ_1 = 0.03 W/(m K)
- panel skins : thicknesses $s_2 = s_4$ = 1 mm , conductibility λ_2 , λ_4 = 150 W/(m K)
- panel core : honeycomb/paraffin condensate of thickness s_3 = 38 mm with an effective conductibility λ_3 , where:

λ_3 = filling efficiency x $\lambda_{paraffin}$ + honeycomb volume fraction x λ_{Al}

λ_3 = 0.82 x 0.45 W/(m K) + 0.03 x 200 W/(m K))

λ_3 = (0.4 + 6) W/(m K)

- and an additional contact resistance $R_{contact}$ between skins and panel core due to the honeycomb adhesive film. It is difficult to establish this resistance a priori. We found a reasonable agreement with measurements (see section 5) after assuming:

$R_{contact} = 3\ 10^{-3}$ K m^2/W

The window is then subjected to disturbances of different spatial frequencies with input stimuli proportional to cos *ky*, where *y* is the spatial coordinate (Fig. 2) and *k* is the wave number (the disturbance wavelength being therefore $L = 2\ \pi / k$). We test separately three types of stimuli :

- a wavy temperature on the foam edge
- a wavy heat generation on the heating pad
- a wavy surface loading from convection

Due to the linear behaviour , the temperature response of the external face T_{face} is also proportional to cos *ky*. The B stimulus is actually a power per unit surface and the response is normalized with the resistance s_1 / λ_1 to give a 'temperature'. Similarly the C stimulus is a power per unit surface and the response is normalized with the resistance

$$s_1 / \lambda_1 + s_2 / \lambda_2 + R_{contact} + s_3 / \lambda_3 + R_{contact} + s_4 / \lambda_4$$

Fig. 3 shows the trace for a stimulus of unit ripple amplitude on T_{face} as a function of the stimulus frequency. One observes a very efficient INHERENT suppression of the disturbances with wavelengths of decimetres . There is apparently no need for a fine heating control segmentation. This is also confirmed by the stratification simulation presented in section 2.5.

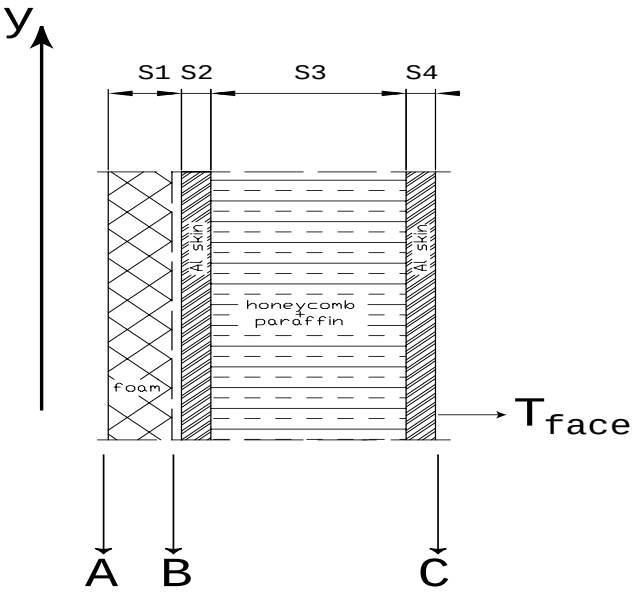

Figure 2: Schematic thickness build-up of Preshower (SE) window. SE inside - cold - to the left. Heating pads are located between insulating foam and window panel. Of interest is to obtain an accurate, constant and uniform exterior temperature T_{face} (right).

a. Details concerning this procedure and the appropriate equations may be found in [2].

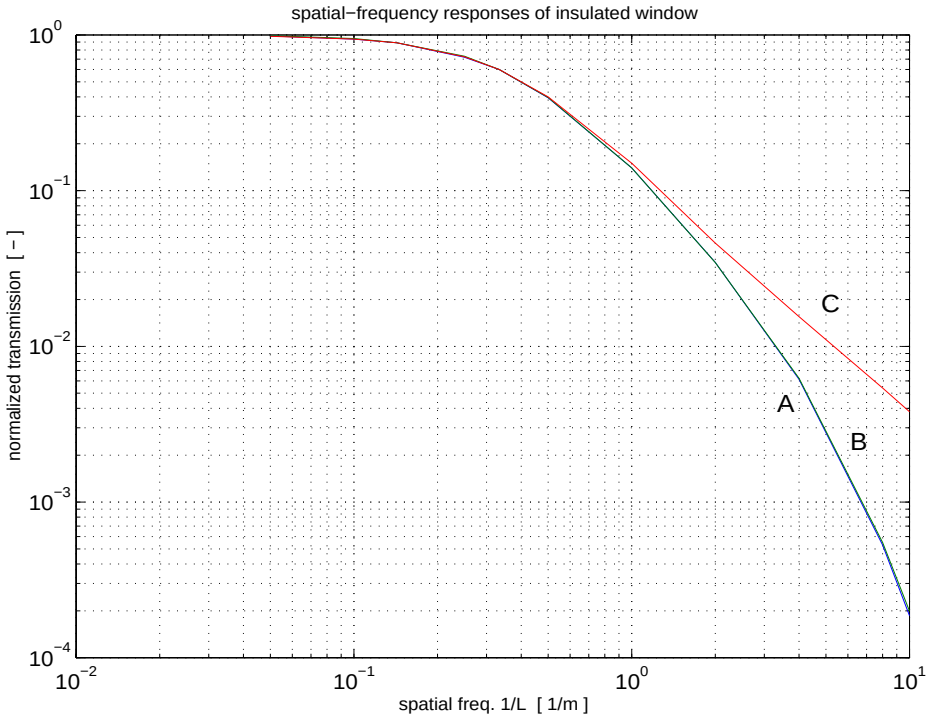

Figure 3: Amplitude of the ripple on the profile of the temperature of interest T_{face} for three different disturbance scenarios A, B and C. The latter is 'nearby', and consequently its spectrum is somewhat 'harder'.

2.3 Proposed control layout

The spatial granularity of the proposed control results from the observations reported in the previous section. The heating pads (foils) are placed on the window's inside. Each window comprises 12 identical foils per window, divided in an upper block (6) and a lower block (6). There is 1 feedback loop for the upper block, and 1 for the lower block. Each foil is equipped with 2 temperature sensors (for example PT100) which are also on the window's INSIDE for reasons which will be explained in the next section.

The feedback signal of the upper block is obtained from the average value of the upper 2 x 6 temperature readings, and similarly for the lower block.

The foils are built from Cu cladding on a polyimide foil. The typical power rating is 84 W/m^2 but the design rating is 260 W/m^2 with a 48 V supply budget.

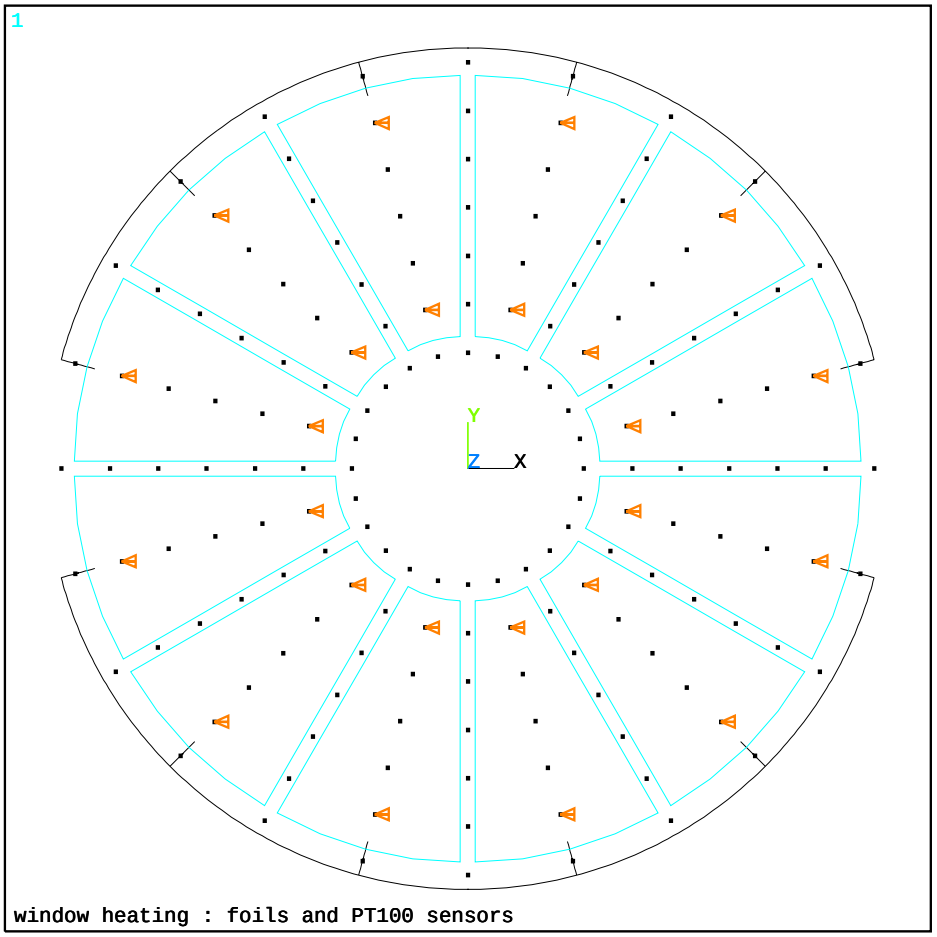

Figure 4: Schematic layout of heating pads on window surface, grouped together into an upper and a lower block. The dots represent the nodes of the finite element model. The arrows indicate the position of the temperature sensors used in the model. The average of the readings of the 12 uppermost sensors is the 'upper' temperature, and similarly for the 'lower' temperature.

2.4 Dynamic thermal behaviour of the window and consequences on the control system

In the proposed layout, the 'plant' (the thing to be controlled) has, from a control point of view, 2 degrees of freedom (DOF) , as shown in the following schematic

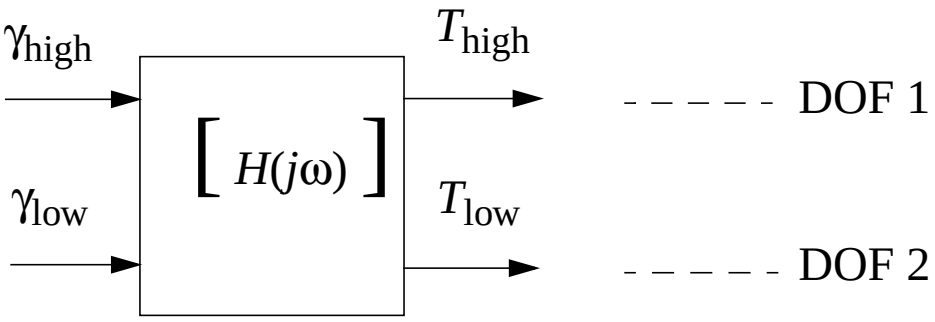

where γ is the applied heating pad power per unit area and T is obtained from the average of the thermal sensors readings.

[H] is the frequency response matrix :

$$[H] = \begin{bmatrix} H_{11} & H_{12} \\ H_{21} & H_{22} \end{bmatrix}$$

From symmetry :

$$H_{11} = H_{22} \qquad H_{12} = H_{21}$$

The diagonal element H_{11} is the (averaged) temperature of the *upper* block due to heating of the *upper* block, while the off-diagonal element H_{21} is the (averaged) temperature of the *lower* block due to *upper* block heating. The off-diagonal terms represent *an interaction* (cross-talk), making the plant *multivariable*.

The frequency responses have been estimated by computation in a 3D finite element modelling of the true window (exploiting left/right symmetry) subjected to harmonic 'testing'. The grid density through the thickness has been carefully chosen. The reliability of results decreases for increasing frequency.

The complex components of *[H]* (amplitude and phase) are shown in Fig. 5 as a function of the excitation frequency. We have also made simulations in the case where the temperature sensors would be put on the outside of the window.

One can conclude:

- a feedback based upon measurements on the outside face is not optimal. The exterior temperature response suffers from an important transmission handicap. The corresponding phases continue to 'turn away' for increasing frequency (not plotted), a typical signature of propagation time. This may lead to instability of the closed-loop system
- there is a good amplitude separation (the off-diagonal element is one order of magnitude smaller than the diagonal one) showing little interaction between the upper and lower blocks. As a consequence, *a multivariable controller is not necessary*
- a closed-loop bandwidth of a few mHz is achievable with safety , leading to a straightforward controller design (little or no derivative action is needed)
- the controller gain can be established : a gain of 300 W/(m^2 K) gives a closed-loop bandwidth of a few mHz

2.5 Stratification

The proposed control granularity with only 2 DOFs is quite coarse. Moreover, the SE tank is a fairly tall device. It is therefore legitimate to ask what happens if the SE neighbouring environment (gaseous) has a vertical temperature gradient. Is the window control system able to cope ?

To answer this question, we have run simulations assuming a drastic temperature profile (2 degrees too cold at the bottom, 2 degrees too hot at the top, reference +18˚C respected at beam level). We assume furthermore *unobstructed* convection in the outer space, as shown in Fig. 6.

With T_{cold} = -10˚C , with the same numerical values as in section except for s_4 = 3 mm (1 mm window + 2 mm EE curtain) and with the control layout proposed before, we obtain the temperature profile on the skin/curtain from the finite element model shown in Fig. 7.

The resulting heating actions are :

γ_{high} = 71.24 W/m^2 γ_{low} = 96.76 W/m^2

One observes that the problems (in terms of temperature gradients) are reduced by a factor of 3. In CMS, this factor will be >> 3 since the convection will be obstructed due to the very small space between EE and SE and therefore the film coefficient α will be <<15 W/(m^2 K).

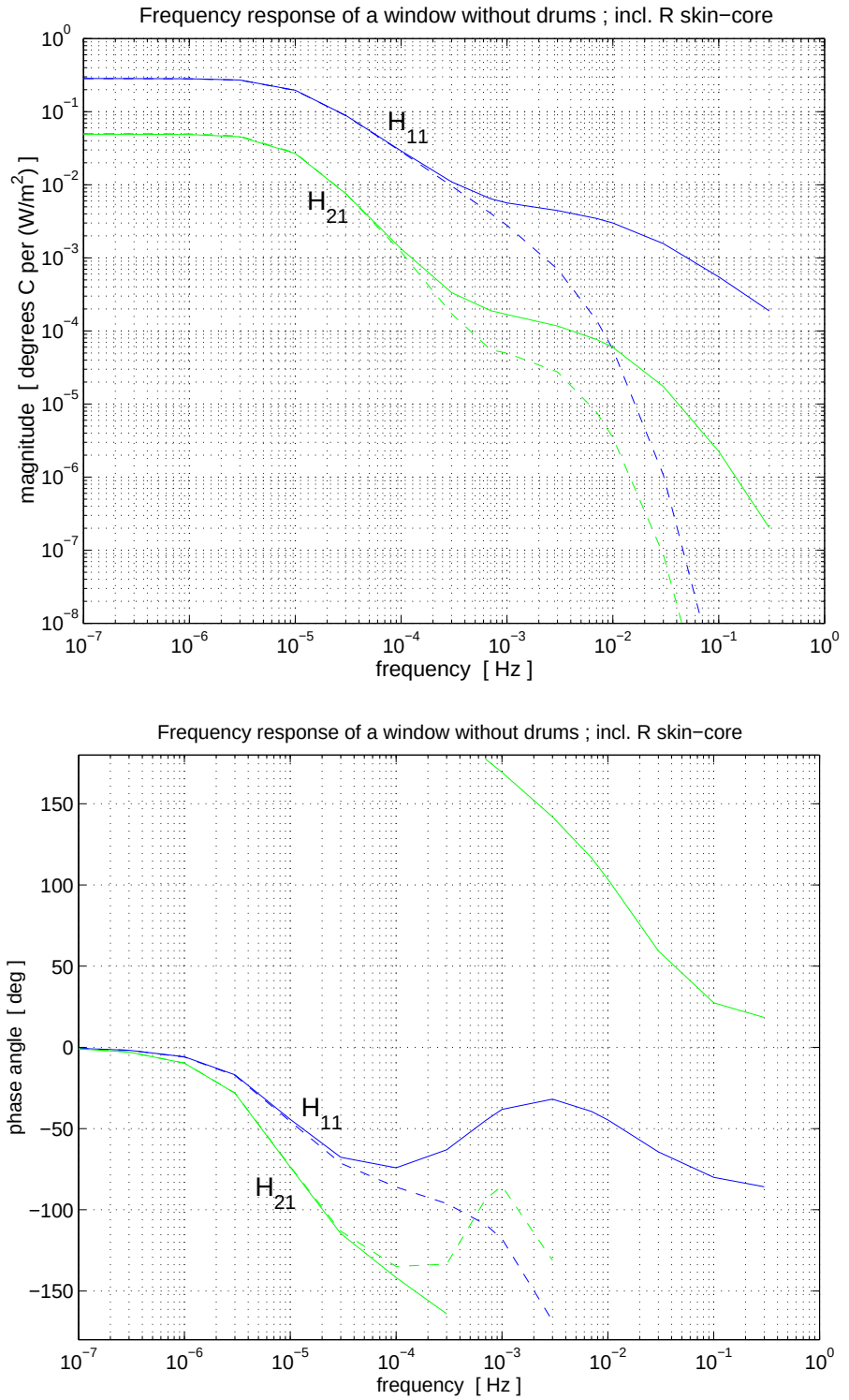

Figure 5: Frequency responses from 3D finite element modelling. Solid : inside response, signal obtained from PT100 averaging. Dashed : response if the temperature sensors would be on the outside.

.

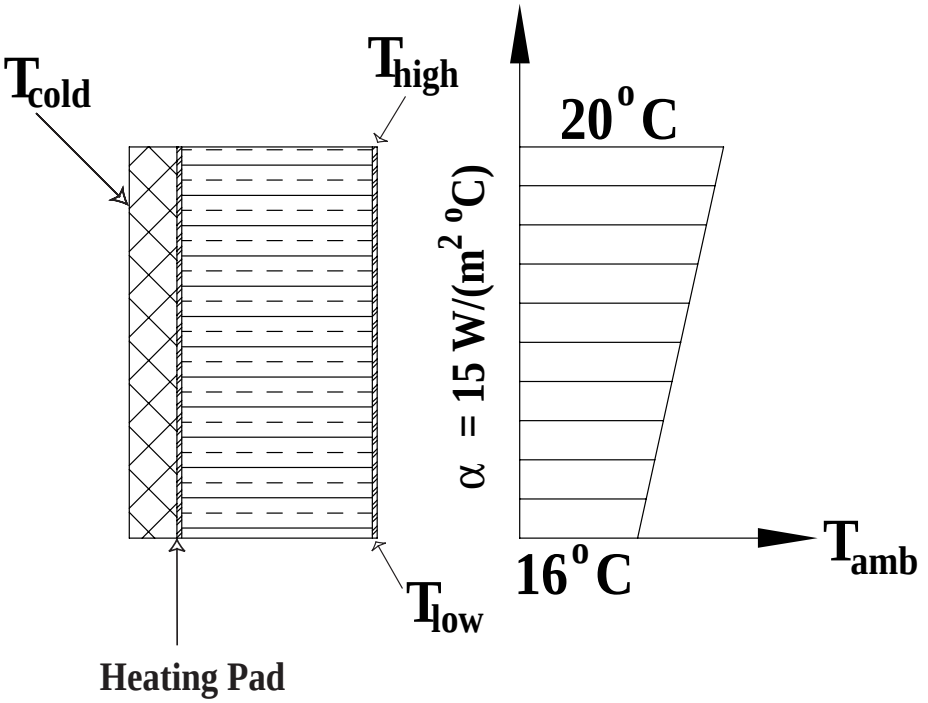

Figure 6: Stratification model (Window thickness and diameter not to scale !)

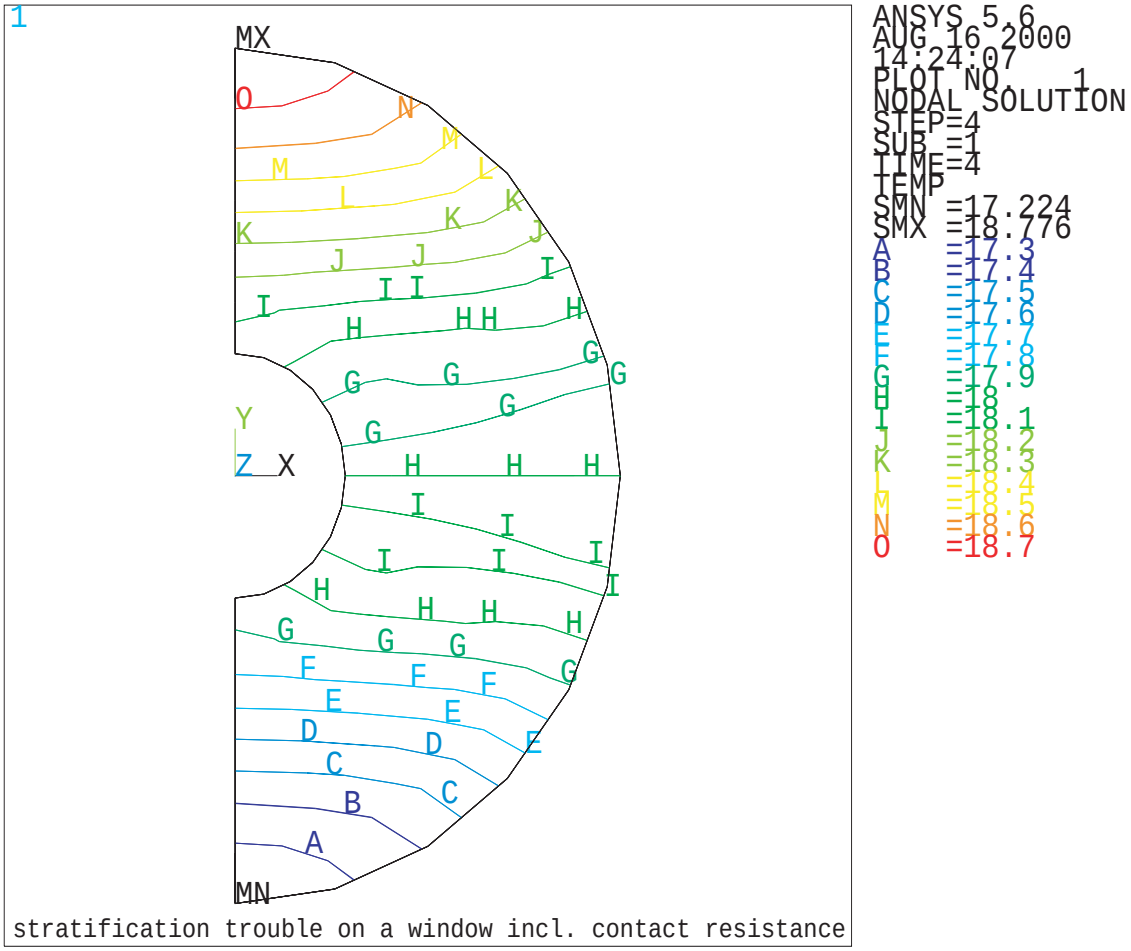

Figure 7: Temperature profile on a window's outer skin subjected to an important convention / stratification attack.. This is the 'rear view' on a true 3D model. Left / right symmetry has been exploited.

2.6 First conclusions on window regulation

The proposed control segmentation (with an upper and a lower block) seems sufficient. A finer segmentation would not only increase the number of DOFs, but would make the multivariable character far more important (so that it can no longer be neglected) and the complexity would explode.

2.7 Dynamic model of the 'plant'

In the following we present a simple model enabling us to examine how fast the window responds to changes in heating pad power (the nominal input) and to changes in heat load inside and outside of SE (these are disturbances from a control viewpoint).

We have learnt from the H_{11}/H_{21} amplitude separation that surface non-uniformities do not seem to play an important role in the window's dynamic behaviour. We will therefore make a one-dimensional model describing the conductive and capacitive properties of the window's thickness lay-up. Therefore, all quantities below will be specific, i.e. per unit surface area.

The insulating foam can be approximated as a pure resistor (without capacitance), and the panel skins can be taken as pure capacitors (remember that we only treat through-thickness phenomena) . The panel core has to be seen as a transmission line, a body with dispersed conductance and capacitance. It is in our interest to try and approximate this line with a discrete (lumped) model in a classical way, i.e. with a series connection of unit cells. Doing so, we no longer need finite elements, we simply obtain a linear network as shown in Fig. 8.

Let us introduce *C*, the capacitance per unit area, and resistance *R* (the inverse of which is the conductance per unit area). Let us compute these quantities for each part of the network.

The foam is taken to be a pure resistor

$$R_f = \frac{s_{foam}}{\lambda_{foam}} = \frac{1\times10^{-2}\ \text{m}}{3\times10^{-2}\ \text{W/(m K)}} = \frac{1}{3}\ \text{m}^2\text{K/W}$$

The window skin is assumed to be a pure capacitor

$$C_s = \rho_{Al} \cdot c_{Al} \cdot s_{skin} = 2700\ \text{kg/m}^3 \cdot 900\ \text{J/(kg K)} \cdot 1\times10^{-3}\ \text{m} = 2.43\times10^3\ \text{J/(m}^2\text{K)}$$

There is a contact resistance between the skin and the core of the window $R_{contact} = 3\text{x}10^{-3}\ \text{m}^2\text{K/W}$ as mentioned previously.

The core is a transmission line, approximated as a series connection of *n* unit cells R_l - C_l

where $R_l = R_{core} / n$ and $C_l = C_{core} / n$

$$R_{core} = \frac{s_{core}}{\lambda_{eff-core}} = \frac{40\times10^{-3}\ \text{m}}{6.4\ \text{W/(m K)}} = 6\times10^{-3}\ \text{m}^2\text{K/W}$$

$$C_{core} = (\eta_{moderator} \cdot \rho_{paraffin} \cdot c_{paraffin} + \rho_{honeycomb} \cdot c_{Al}) \cdot s_{core}$$

$$= (0.82 \cdot 950\ \text{kg/m}^3 \cdot 1880\ \text{J/(kg K)} + 82\ \text{kg/m}^3 \cdot 900\ \text{J/(kg K)}) \cdot 40\times10^{-3}\ \text{m}$$

$$= 6.15\times10^4\ \text{J/(m}^2\text{K)}$$

The nominal input is a current source *i* representing heating pad power (per unit area) (it corresponds to what we called γ in section 2.4).

The disturbances are represented by

- a voltage source *v'* representing SE inside (cold) temperature
- a current source *i'* representing the external surface power attack (convection)

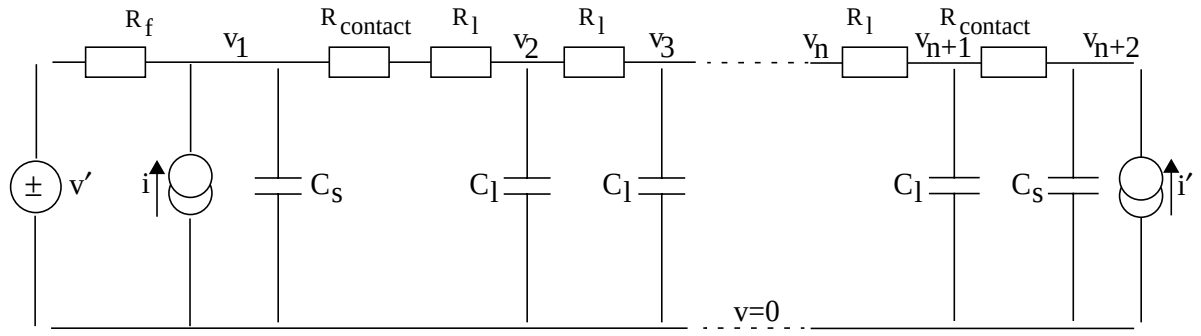

Figure 8: Linear network representing a discrete approximation of the window's through-thickness build-up, with the 3 possible stimuli.

Writing down the network's equations in the state-space format does not involve too much burden. With the classical notations (the dot denotes time derivative) :

$$\{\dot{x}\} = [A] \cdot \{x\} + [B] \cdot \{u\}$$
$$\{y\} = [C] \cdot \{x\} + [D] \cdot \{u\}$$

and with the state vector , input vector and output vector respectively :

$$\{x\} = \begin{bmatrix} v_1 \\ v_2 \\ v_3 \\ \cdot \\ \cdot \\ v_n \\ v_{n+1} \\ v_{n+2} \end{bmatrix} \qquad \{u\} = \begin{bmatrix} i \\ v' \\ i' \end{bmatrix} \qquad \{y\} = \begin{bmatrix} v_1 \\ v_{n+2} \end{bmatrix}$$

one obtains :

$$[A] = \begin{bmatrix} \beta & \gamma & 0 & & & & & & 0 \\ \delta & \varepsilon & \zeta & 0 & & & & & \\ 0 & \alpha & -2\alpha & \alpha & 0 & & & & \\ & 0 & \alpha & -2\alpha & \alpha & 0 & & & \\ & & \cdot & \cdot & \cdot & \cdot & \cdot & & \\ & & & \cdot & \cdot & \cdot & \cdot & \cdot & \\ & & & & 0 & \alpha & -2\alpha & \alpha & 0 \\ & & & & & 0 & \alpha & -2\alpha & \alpha & 0 \\ & & & & & & 0 & \alpha & \eta & \theta \\ 0 & & & & & & & 0 & \kappa & -\kappa \end{bmatrix} \qquad [B] = \begin{bmatrix} \mu & \nu & 0 \\ 0 & 0 & 0 \\ . & . & . \\ & & \\ & & \\ & & \\ & & \\ . & . & . \\ 0 & 0 & 0 \\ 0 & 0 & \mu \end{bmatrix}$$

$$[C] = \begin{bmatrix} 1 & 0 & . & & & & & . & 0 & 0 \\ 0 & 0 & . & & & & & . & 0 & 1 \end{bmatrix} \qquad [D] = \begin{bmatrix} 0 & 0 & 0 \\ 0 & 0 & 0 \end{bmatrix}$$

where :

$$\alpha = \frac{1}{R_l \cdot C_l} \qquad \beta = -\frac{1 + \dfrac{R_f}{R_{contact} + R_l}}{R_f \cdot C_s} \qquad \gamma = \frac{1}{(R_{contact} + R_l) \cdot C_s}$$

$$\delta = \frac{1}{den} \qquad \varepsilon = -\frac{2 + \dfrac{R_{contact}}{R_l}}{den} \qquad \zeta = \frac{1 + \dfrac{R_{contact}}{R_l}}{den}$$

$$\eta = -\frac{1 + \dfrac{R_l}{R_{contact}}}{R_l \cdot C_l} \qquad \theta = \frac{1}{R_{contact} \cdot C_l} \qquad \kappa = \frac{1}{R_{contact} \cdot C_s}$$

$$\mu = \frac{1}{C_s} \qquad \nu = \frac{1}{R_f \cdot C_s} \qquad den = (R_{contact} + R_l) \cdot C_l$$

In the steady-state there are no capacitor currents. If furthermore the current sources *i* and *i'* are silent, then all nodal voltages (state variables) are the same and equal *v'*. This gives an interesting test on the sum of the entries of each individual row of [*A*].

The first output variable (v_1 = internal skin temperature) will be plotted in solid line, and the second (v_{n+2} = external skin temperature) in dashed line, as we have done before.

We have taken $n = 20$, which is adequate for the frequency range of interest.

It is particularly easy, efficient and numerically safe to study such a system with the MATLAB [3] software. A selection of the results is given in Fig. 9. Only the response to the nominal input is given. This information is necessary for controller design. The responses to the other inputs (disturbances) are not very meaningful in open loop. These inputs have been included in the model in order to be prepared for closed loop studies.

The fact that one cannot cool with the heating pads, and thus not give an AC stimulus, is only a hypothetical problem, knowing that, in real life, the heating will always contain an important DC offset.

It is implicitly understood that only one stimulus at the time is switched on. Here we thus have the temperature at SE cold inside 'zero' and no external power transfer, which means that the window external face is insulated.

For very low frequencies, we deal with the static limit case where the window is isothermal through its thickness. No thermal flux crosses the window because of the insulation condition on the outside. The temperature is entirely determined by the foam's resistance.

In the mid-frequency range we approximately have an integrator[a)]. The heating power now serves to oscillate the window's temperature rather than it being transmitted through the foam. The window can still be approximated as being isothermal (internal and external responses do not yet differ significantly), and thus as a capacitor with value:

$$C_{total} = C_s + C_{core} + C_s = 6.636 \times 10^4 \ \text{J/(m}^2\ \text{K)}$$

The border between low- and mid-frequency ranges is given by a take-over frequency:

$$f_{break} = \frac{1}{2\pi R_f C_{total}} = 7.2\ \mu\text{Hz}$$

which corresponds approximately to the lowest eigenvalue of [*A*] .

In the high-frequency regime, more and more of the transmission line becomes decoupled, in the sense that the stimulus no longer 'feels' it. It becomes gradually harder to pump anything down the line; the magnitude of the *external* response decreases very rapidly with increasing frequency. The internal and external responses deviate away from each other. The spectrum for the *internal* response becomes 'harder', the phase lag shows recovery :

a. an integrator features a -1 (decade per decade) slope in a double-log magnitude plot, and a 90 degrees phase lag

inertia is being decoupled. The phase of the *external* response completely turns away, which is typical for propagation time phenomena. The non-negligible value of the contact resistance $R_{contact}$ results in an early onset of decoupling phenomena.

For very high frequencies, everything but the internal skin is decoupled, again resulting in an integrating behaviour.

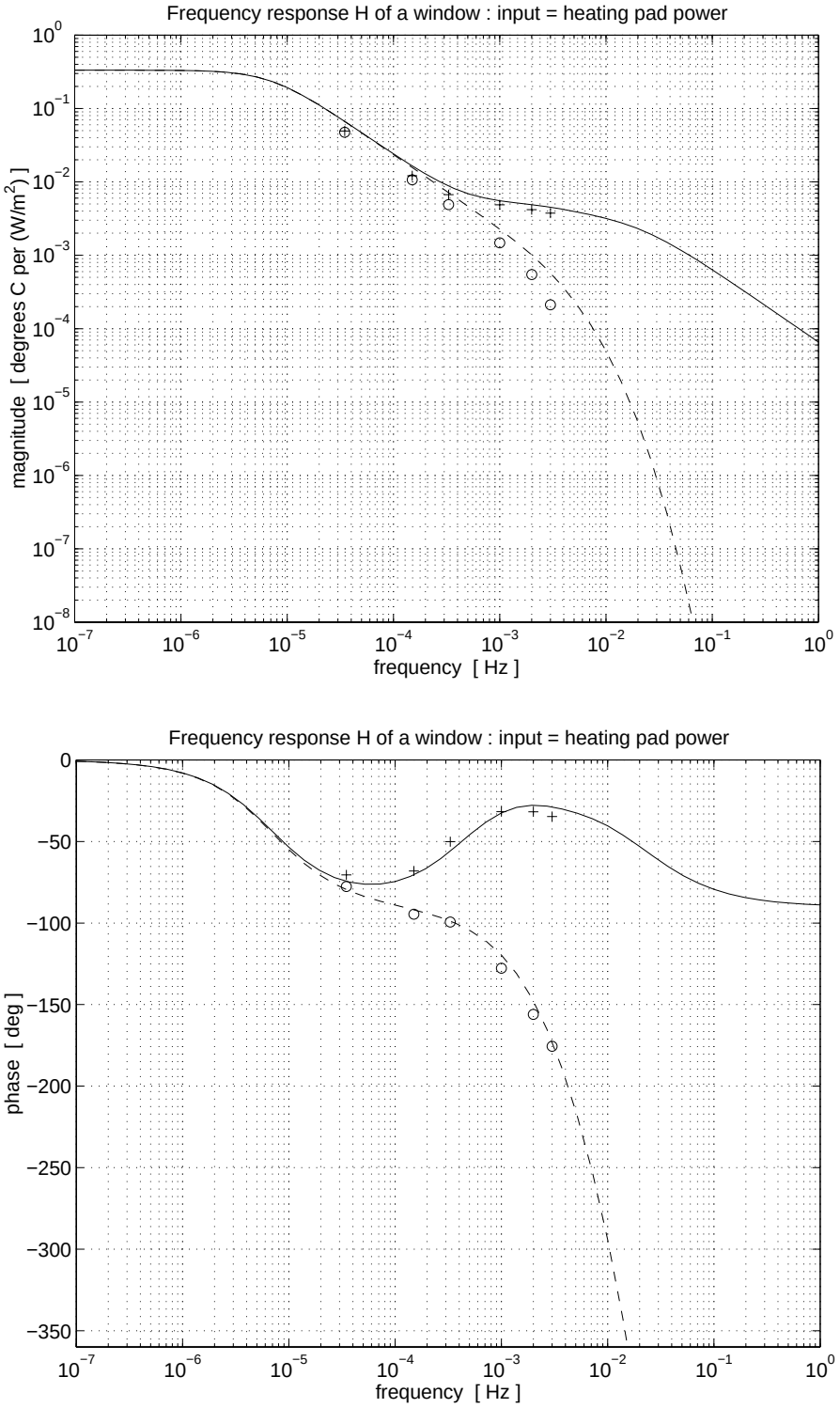

Figure 9: Response of the model to heating pad stimulus, confronted with the measurements on the 1 * 0.5 m^2 prototype (see section 5). Edge effects are non-negligible on this small device.

2.8 Controller design & computed closed-loop behaviour

See [2] for information on control theory. We propose a PI controller (proportional-integrating) with a transfer function :

$$G(s) = M \cdot \left(1 + \frac{1}{\tau_i \cdot s}\right)$$

where :

- s = Laplace variable
- M is the gain M = 300 W/(m^2 K)
- integrating-to-proportional take-over frequency : $\frac{1}{2\pi\tau_i} = 0.1$ mHz

Upon feeding-back the actual temperature T (internal skin - obtained by averaging) and comparing it with the desired value or setpoint T_{set}, the error signal T_ε is obtained. The controller acts upon this error signal (Fig. 10). The possible stimuli are now :

- the setpoint (variations)
- the two afore-mentioned disturbances.

As before, testing the response to one stimulus implicitly understands that the other two are quiet.

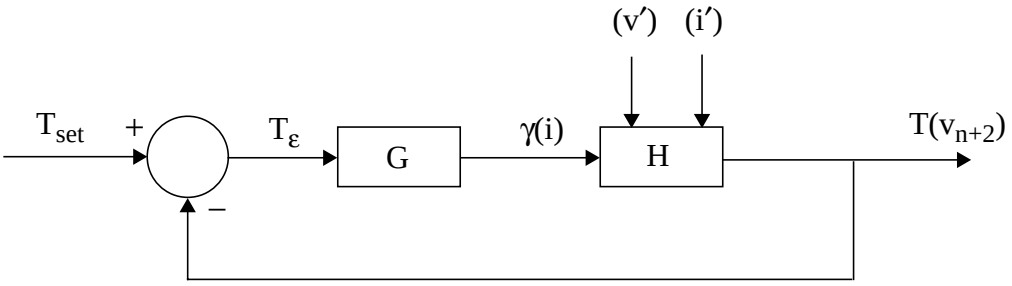

Figure 10: The feedback loop scheme, with controller G and plant H . The notations used in the network model are in brackets.

The frequency and transient (time) responses are again obtained with MATLAB. The results are presented in Fig. 11 to Fig. 13. One notes that:

- Within a certain frequency band, the loop's *bandwidth*, it is feasible to follow adequately the set point variations. Beyond this band, this task becomes gradually more difficult. This feature is typical for all real-life feedback systems.
- For very low frequencies, the disturbance rejection is enhanced by the controller's integrating action. For high frequencies, it is the plant's own inertia which makes the system less vulnerable. The low-frequency *external* response to an *external* disturbance is limited by the windows thermal conductance rather than by the controller's performance. However, even this limited rejection should be adequate, taking into account possible orders of magnitude for external disturbances; see section 2.5.
- Many transient responses show a 'fast component', related to the plant's very-high-frequency behaviour.

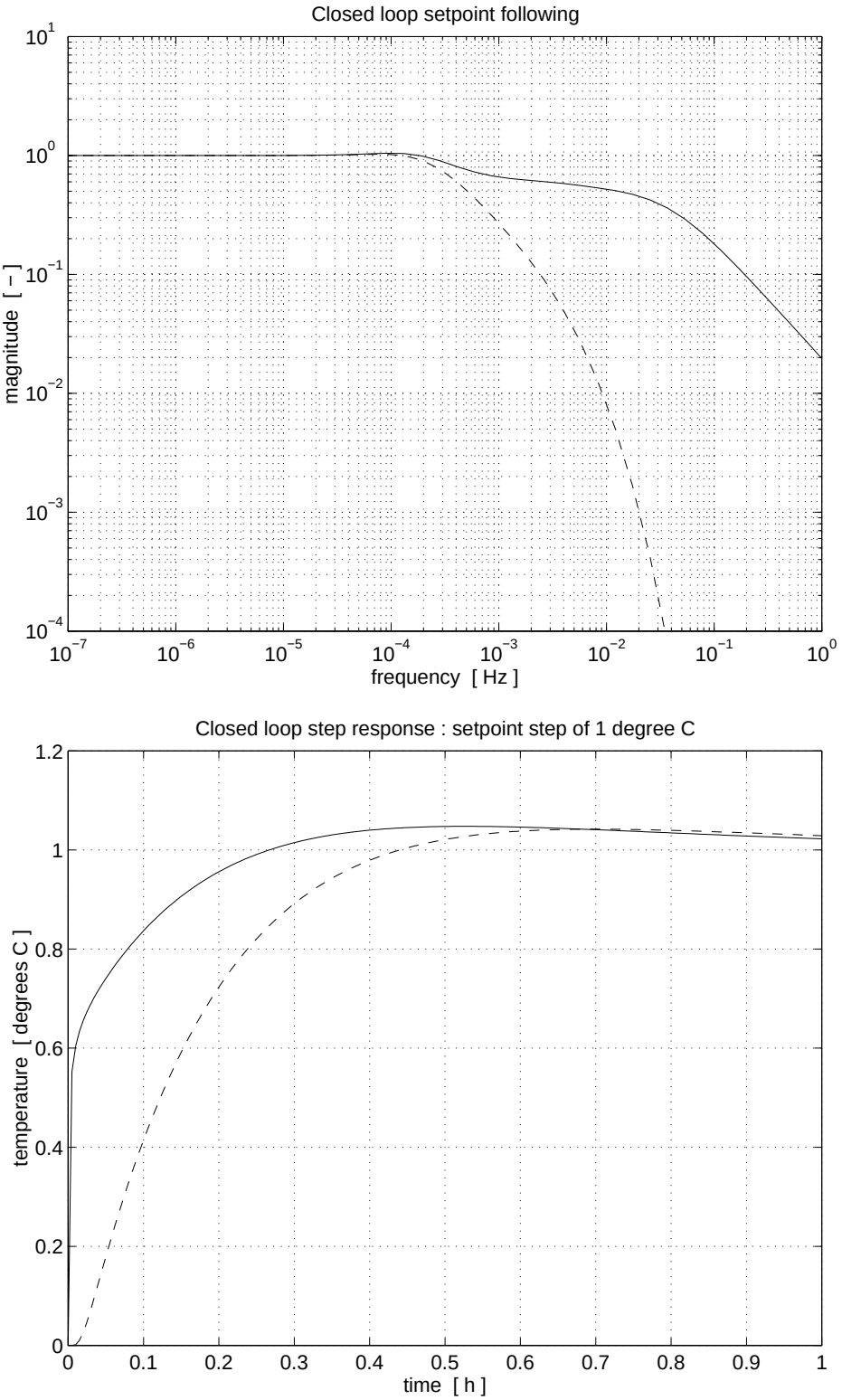

Figure 11: Set point following of the closed-loop system

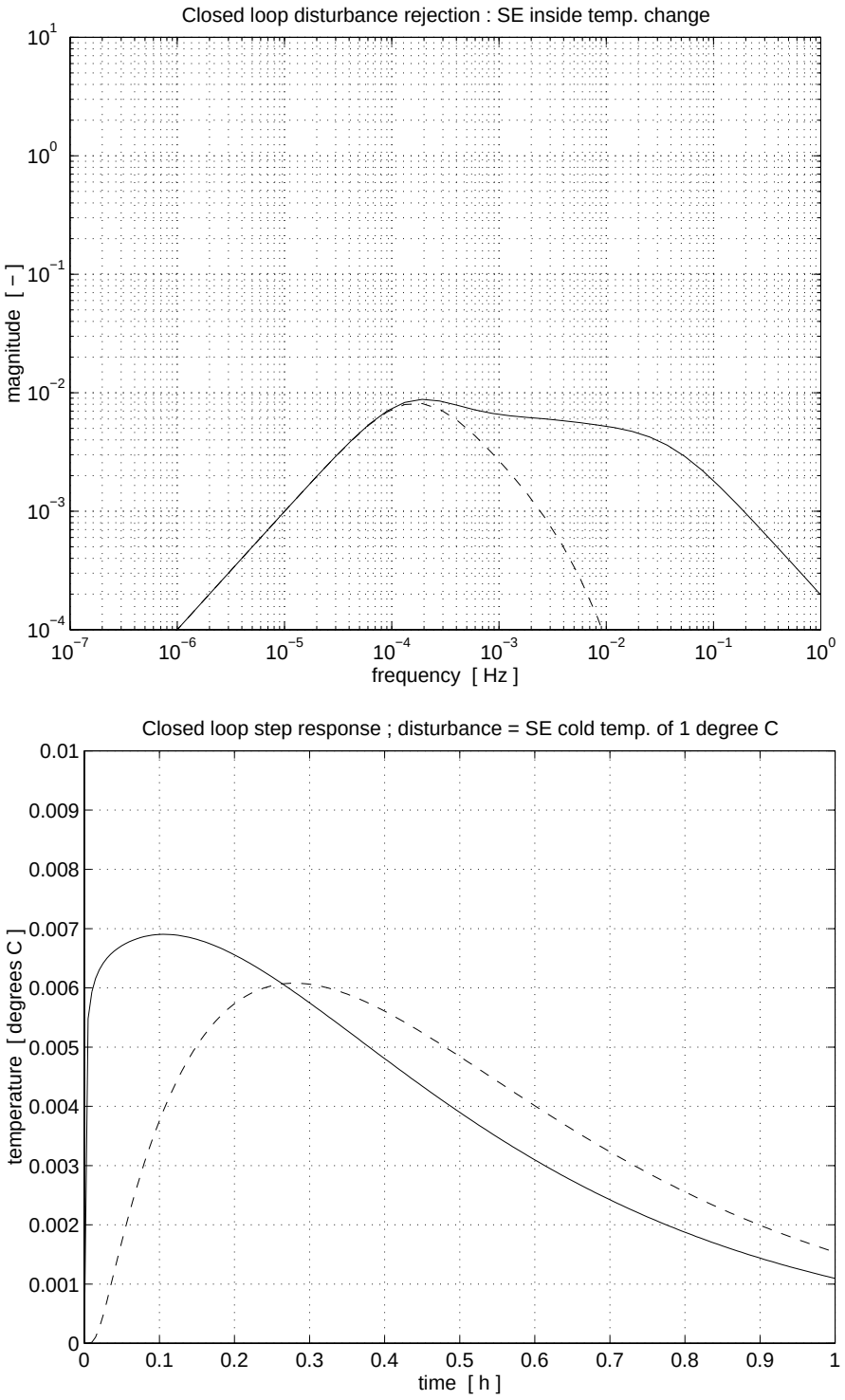

Figure 12: Response of the closed-loop system to variations in SE internal (cold) temperature.

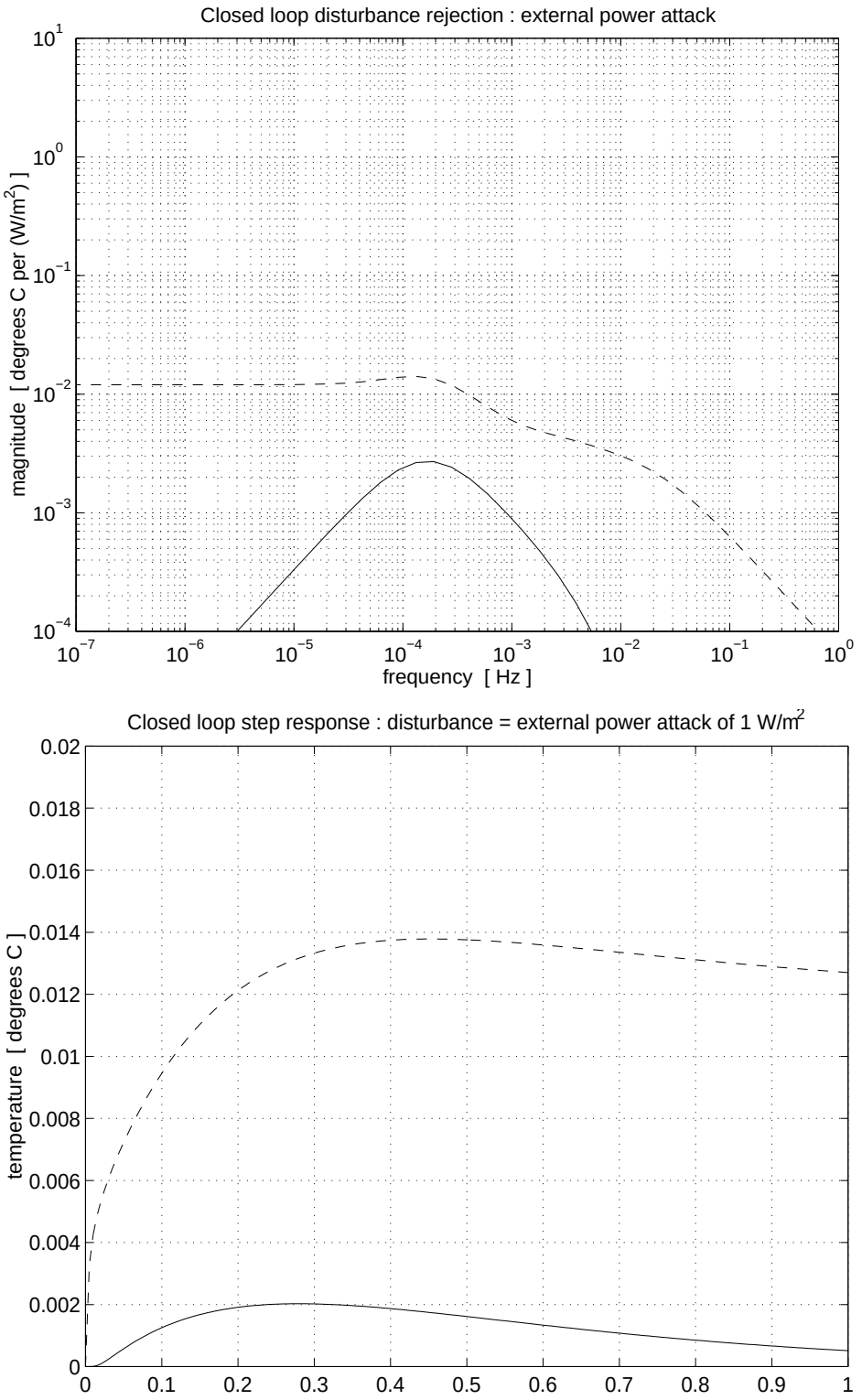

Figure 13: Response of closed-loop system to external attack.

3 The Window prototype setup

The size of the prototype Preshower window is 50cm x 100cm. The structure of this model is identical to the final Preshower window which has been described in section 2.1. It has been filled with paraffin using the same procedure and the same tooling as developed for the final product. A prototype of the heating film (shown in Fig. 14) is taped onto the internal face of the window. It consists of three embedded copper conductor circuits of identical length, encased in polyimide foils, whose geometry is optimized to provide a uniform heating power when the three conductors are connected in parallel. The resistance seen from the heating film power supply is 4.6 ohms.

A schematic of the setup is shown in Fig. 15 whilst a photograph is shown in Fig. 16. The external face of the window is presented towards the external environment. The internal face is separated from cooling elements (which represent the cold inside of the Preshower) by a 8mm thick Rohacell plate. The cooling elements consist of 1mm thick copper plates soldered to copper tubes in which circulates a cooling fluid. A thermostatically controlled cooling device with a maximum cooling power of ~100W regulates the input temperature of the cooling fluid with a stability better than 0.1°C. The whole setup is encased in a wooden box lined with 5cm thick polystyrene foam such that all the faces except the external face of the window are thermally insulated.

The temperature of the window's internal face is monitored by four PT100 probes glued to the aluminium skin (small holes in the heating film ensure that the probe measures the skin temperature and not the heating conductor or polyimide temperature). The probes are positioned regularly along the longest dimension with a pitch of 20 cm. The temperature of the external window skin is monitored by three PT100 probes, separated by 30cm. The temperatures of the copper cooling block, of the input and output coolant and the ambient temperature close to the set-up are also monitored. The difference between input and output coolant temperature was always smaller than 0.5°C.

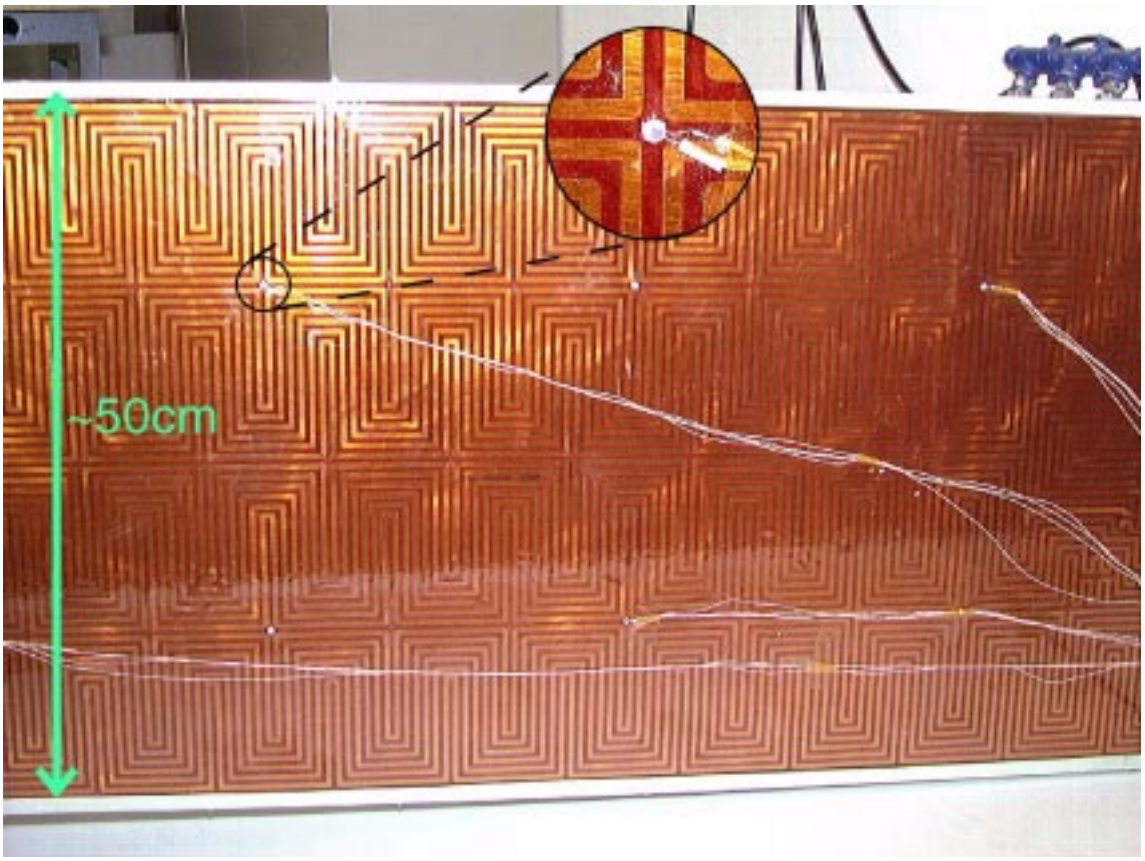

Figure 14: Photograph of the heating film. The inset shows a close-up of one of the temperature sensors placed on the film.

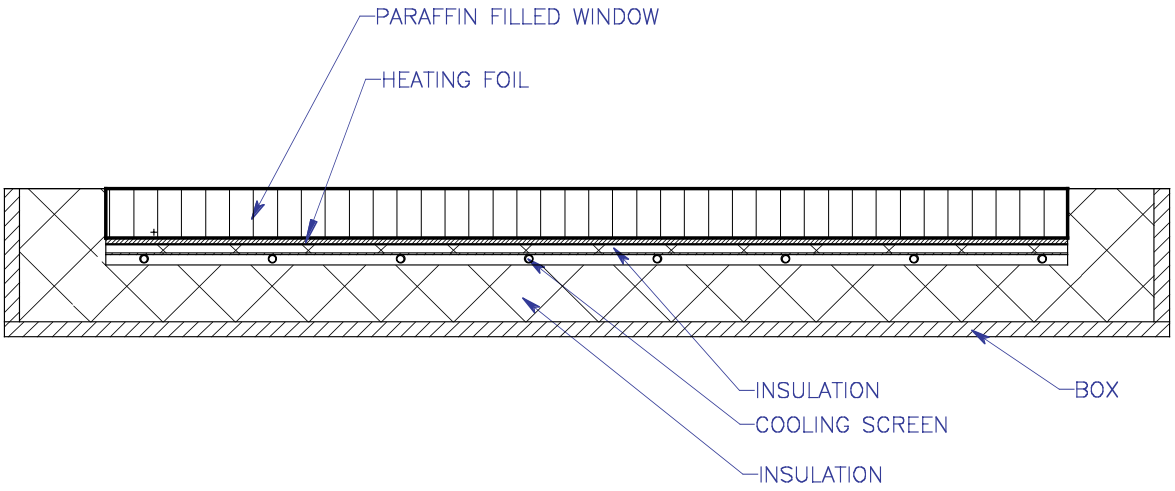

Figure 15: Schematic diagram showing the experimental setup

Figure 16: Setup of the window prototype

The temperature measurement accuracy (i.e. the quantification step) with the hardware described in the next section is 0.006°C . The measurement noise (= short term variation) was very small (less than 0.1°C peak to peak) except for the probe measuring the room temperature which showed a larger fluctuation (0.3°C peak-to-peak) for unknown reasons. The temperature measurement showed very good short and medium term (several days) stability, well within 0.1°C.

However, we observed on a few occasions a sudden change of one probe relative to the others of up to 0.5°C. These calibration changes were not of concern for our regulation measurements (which lasted at maximum a few days) but prohibited us from making a good absolute calibration of the probes and therefore to study in detail the uniformity of the temperature on the window face. These effects certainly require further work to understand whether they are due to the PT100 itself or to the measurement setup.

4 The Regulation System

The regulation system proposed in section 2, using the average of the inside skin temperatures as input to the feedback loop, has been implemented on the window prototype.

The realization has been possible with the use of industrial equipment. No hardware development was necessary. Furthermore, the complete installation has been made with off-the-shelf equipment.

However, the study of the dynamic behaviour of the temperature regulation of the Preshower sub-detector required the creation of a complete process control with a SCADA interface. In this section, we describe in detail the complete system. References [4] and [5] were used when designing this system.

4.1 Basic schematic

The setup of the control process is based on the following schematic diagram (Fig. 17).

- A control unit drives, via a POWER CONTROL line, the electrical power injected on the thermal foil located inside the preshower window.
- An accurate measurement of the injected power is done via a POWER MEASUREMENT line.
- The temperatures of various points at the inner and outer surface of the honeycomb structure are measured and via a control loop (PID) a subset of those value are used to control the power supply.
- A Human Machine Interface (HMI) is built with a standard SCADA (Supervisory Control And Data Acquisition) software.

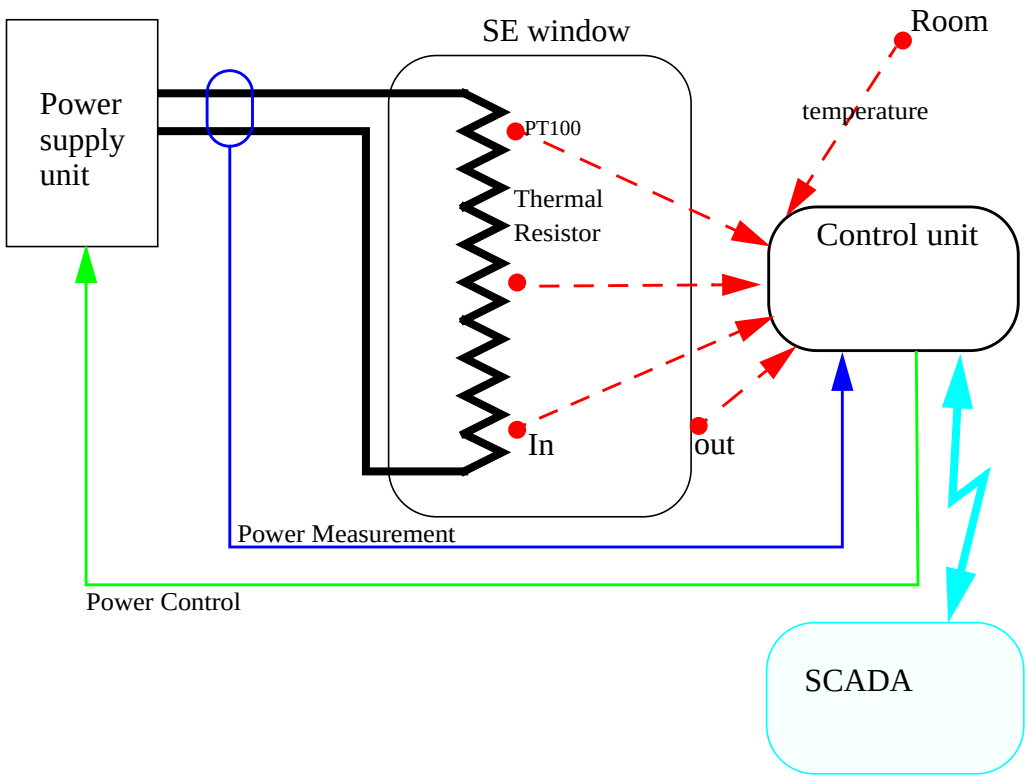

Figure 17: Schematic diagram of the regulation setup

4.2 System architecture

The architecture for the prototype includes three distinct layers.

- The front-end elements are composed of thermal sensors and a power supply unit.
- The process control level at which the actuator and sensor hardware are connected, and the programmable logic controller (PLC) managing the regulation.
- The supervisor level used for the control, the monitoring and the archiving of all events.

4.3 Selected technologies.

The control unit is an industrial product selected from the SIEMENS S7-300 series. It comprises a central processor unit with various I/O modules. The choice of SIEMENS was dictated mainly by the availability of the product within the IT/CO-FE laboratory at CERN.

The thermal sensors are the widely used PT100.

The choice of the power supply was more difficult, but a standard CERN EP pool unit has been selected.

The supervisor unit acting as a SCADA is the *BridgeView* software from NATIONAL INSTRUMENTS running on PC/NT.

Besides the study of the thermal behaviour of the Preshower Windows, this exercise was used to demonstrate the ease of building a complete control system with standard industrial products.

4.4 Hardware products

4.4.1 The power supply.

The regulation of an AC voltage switched by a static relay is a possible solution for the regulation but this raises the major problem of electrical noise. A solution using a DC power supply designed with a continuous remote control of the voltage is more convenient.

The selected model was a DELTA ELEKTRONIKA (SM7020) standardized in the CERN EP pool. The delivery power of this unit is limited by the curve of Fig. 18.

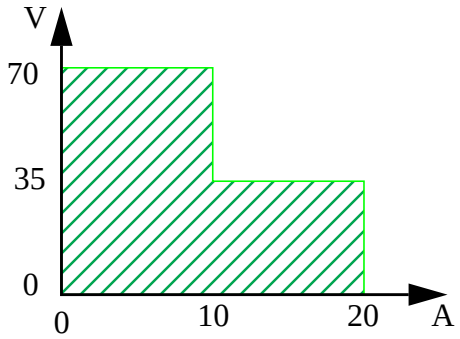

Figure 18: Power limit of the selected power supply

A maximum power of 700 W is available. The remote control of the voltage and the current limitations is possible via 2 channels of 0-5V signals. For this exercise, only the voltage channel is used.

To gain more flexibility in case of the selection of another power supply, the measurement of the voltage applied to the load was done directly via an analogue control channel. The measurement of the current was done by measuring the voltage drop on a serial resistor (0.15 ohms) inserted in the circuit.

The nominal power required for the prototype is around 35 W.[a)] and the thermal foil used has a resistance of 4.6Ω. This gives the required voltage of 7.6 V with a current of 1.6 A.

4.4.2 The control unit.

The complete process control unit is based on a programmable logic controller (PLC) of the SIEMENS S7 -300 series. Attached to this PLC unit there are 3 types of I/O devices.

- One communication interface to the PROFIBUS network.
  This network is used to connect the control unit to the SCADA supervisor. It is a popular network used in the industrial control environment. The choice of this network was mainly imposed by the available IT/CO-FE on shelf equipment.
- One output module with a capability of 4 channels.
- One channel is used to drive the power supply.
- Two Input modules with a capability of 8 channels each.
  Two channels are used to measure the voltage apply to the load and the current passing through the load.
  All the 14 others channels are dedicated for the measure of 7 temperatures sensors based on 4 wires PT100.

a. For a foam of thickness 1cm, surface 0.5m^2 and conductivity 0.03W/(m K) and for a temperature difference of 18 degrees.

4.4.3 Technical capacity of the control unit.

Hardware

The PLC unit has an instruction cycle rate in the range of 0.3 msec per 1000 binary instructions.

The PROFIBUS network is running at a rate of 1.5 Mbits/sec.

The accuracy of the thermal sensor input is in the range of 0.01°C. A noise rejection filter for the 50Hz is applied to each channel.

Software

A complete SIEMENS STEP 7 software development system, running on a Windows™ NT operating system, has been used for the creation of the code.

The code was built with the STANDARD library. This library also provides the necessary function for the control loop module.

4.4.4 The supervisor

The supervisor level is built around *BridgeView* version 2.1 running in a Windows™ NT platform.

A PCI-bus interface was included for communication with the PROFIBUS network.

This connection was done via an APPLICOM PCI1500PFB interface. The goal of this board and its software is to allow the communication between the SCADA and any devices connected to the PROFIBUS network. The communication is based on the standard OPC protocol (OLE for Process Control).

This protocol, running with the Microsoft OLE/COM communication protocol, is specified by the OPC foundation and it is widely accepted by industry. The OPC protocol is a client/server process. The APPLICOM acts as the OPC server.

With the use of this standard, it is possible to have the APPLICOM board located in one PC and the BridgeView SCADA with its OPC client interface installed in another PC. The OPC protocol runs on top of TCP/IP and is transparent in the whole CERN network.

Figure 19 shows a picture of the visual control panel on the PC developed with *BridgeView*.

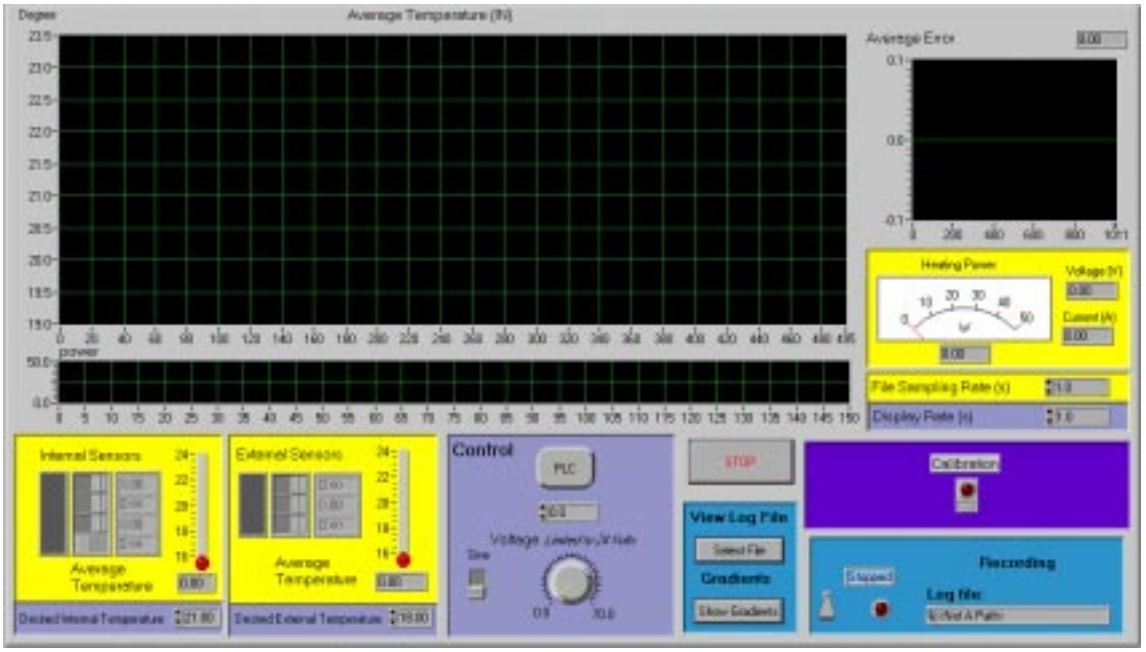

Figure 19: Interface of the monitoring/control program running on the PC

4.5 PLC software configuration.

The software running in the PLC is downloaded from a software development system into a non volatile memory area. In the same manner all parameters coming from the SCADA are stored in a non volatile memory. This provides a complete autonomy of the control unit process. Event after power failure, the process will restart automatically with the last stored parameters.

4.5.1 Configuration data (SCADA/PLC).

Information provided by the scada:

- The offset temperature for the correction and adjustment of the 7 sensors
- The reference temperature (setpoint) expected.
- The Proportional, Integral, and Derivative factors used for the PID algorithm.
- If needed (for test purposes) the voltage value driven by the power supply. In this case, the PID function is interrupted.

Information provided by the PLC:

- The measurement of the 7 temperature sensors with the offset correction.
- The voltage and the current at the heating foil.

4.5.2 Inside the PLC

The program developed in the PLC is quite limited. The size of the code is around 12 kbytes of binary instructions with an additional 9 kbytes reserved for the working area.

- The cycle of the whole process is around 3 msec.
- The control loop function is called every 100 msec for a calculation of a new voltage setpoint.
- The access to the PROFIBUS data queue is done every 100 msec. producing de-facto a sampling rate of 10Hz.
- 2 working modes were possible in the PLC.

Open loop mode

In this mode, the reference voltage for the power supply comes from the SCADA and the control loop is disabled. It is possible to create, from the SCADA supervisor, a *power step* or a *sine wave power* for an evaluation of the dynamic behaviour of the prototype.

Closed loop mode

In this mode, the PLC controller (PID) works with the latest proportional (P), integral (I) and differential (D) values loaded from the SCADA. The PID takes into account the last temperature reference level sent by the SCADA as the setpoint.

The average temperature of internal sensors of the SE window is computed and this value is applied to the PID as the actual temperature. The PID error signal is obtained from the difference to the setpoint. The controller acts on this and produces the required voltage signal to be injected into the power supply.

To secure the configuration, an upper power limitation of 50 W is set in the PLC system and an upper limit of the available current is also imposed via a button located on the front panel of the power supply.

5 Measurement of the frequency response of the window Prototype

The first tests were devoted to measurements of the frequency response of the prototype in open loop, to be compared with the predictions of the dynamic model of section 2.7 and the results shown in Fig. 9. The amplitudes and phases of the response of the internal and external surface temperatures as a function of frequency provide insight into thermal properties of the window, such as the strength of the thermal coupling between the surfaces and its thermal through-conductivity .

The properties of the window prototype were tested by oscillating the heating power in a sine-wave pattern with various frequencies. During the measurement of the thermal responses the external surface of the window prototype was insulated by a thick layer of packing foam from the surrounding environment to avoid effects of the variation of outside temperature on the system.

The period of oscillation of the applied heating power varied from several minutes to eight hours. The measurements of the response lasted, in accordance with the period of the heating power applied, many hours allowing the system to enter into a quasi-steady-state regime of oscillations. A DC power level equal to the oscillation amplitude ensured that the applied power was always positive.

For low frequencies, the amplitude of the heating power was 10W. For high frequencies this amplitude was increased in order to compensate for the decrease of the response and not to be blurred by thermal fluctuations and electronic noise. The response amplitudes were normalized with the amplitude of the heating power applied and the surface area of the window prototype in order to compare the results with simulations of the actual detector. The phases were taken with respect to the phase of the heating power.

Quantitative amplitude and phase information was extracted from the measurements by fitting a system equation to the data. This equation was a sum of a decaying exponential a DC offset and a sinusoidal oscillation. The most important parameters of the fit were the amplitude and phase of the oscillations. The frequency of the oscillations was not a free parameter of the fit and was taken equal to the frequency of the heating power.

The recorded measurements are shown in Fig. 20 for various frequencies of the applied power.

As expected the strong thermal coupling between the two surfaces is visible in the graphs at low frequencies. The difference in amplitude between the inside and outside is relatively small, as is the phase-lag of the response of the external surface with respect to the response of the internal surface.

At higher frequencies the internal and external surfaces decouple thermally: the phase and amplitude of the internal and external face differ substantially.

A comparison of the measurement with the simulations is shown in Fig. 9. The expected internal temperatures are shown as solid lines and the expected external temperatures are shown as dotted lines. The measurements of the internal and external temperatures are shown as crosses and circles respectively.

The agreement between the measurements and the simulations is good. It should be noted that the contact resistance $R_{contact}$ between the skins and the panel core due to the honeycomb adhesive film has been adjusted in the simulation to reproduce best the results. This is however the *only* ‘free parameter’ in the simulation. Furthermore the simulation does not take into account the edge effects of the window prototype which are significant and can account for the remaining disagreement with the measurements.

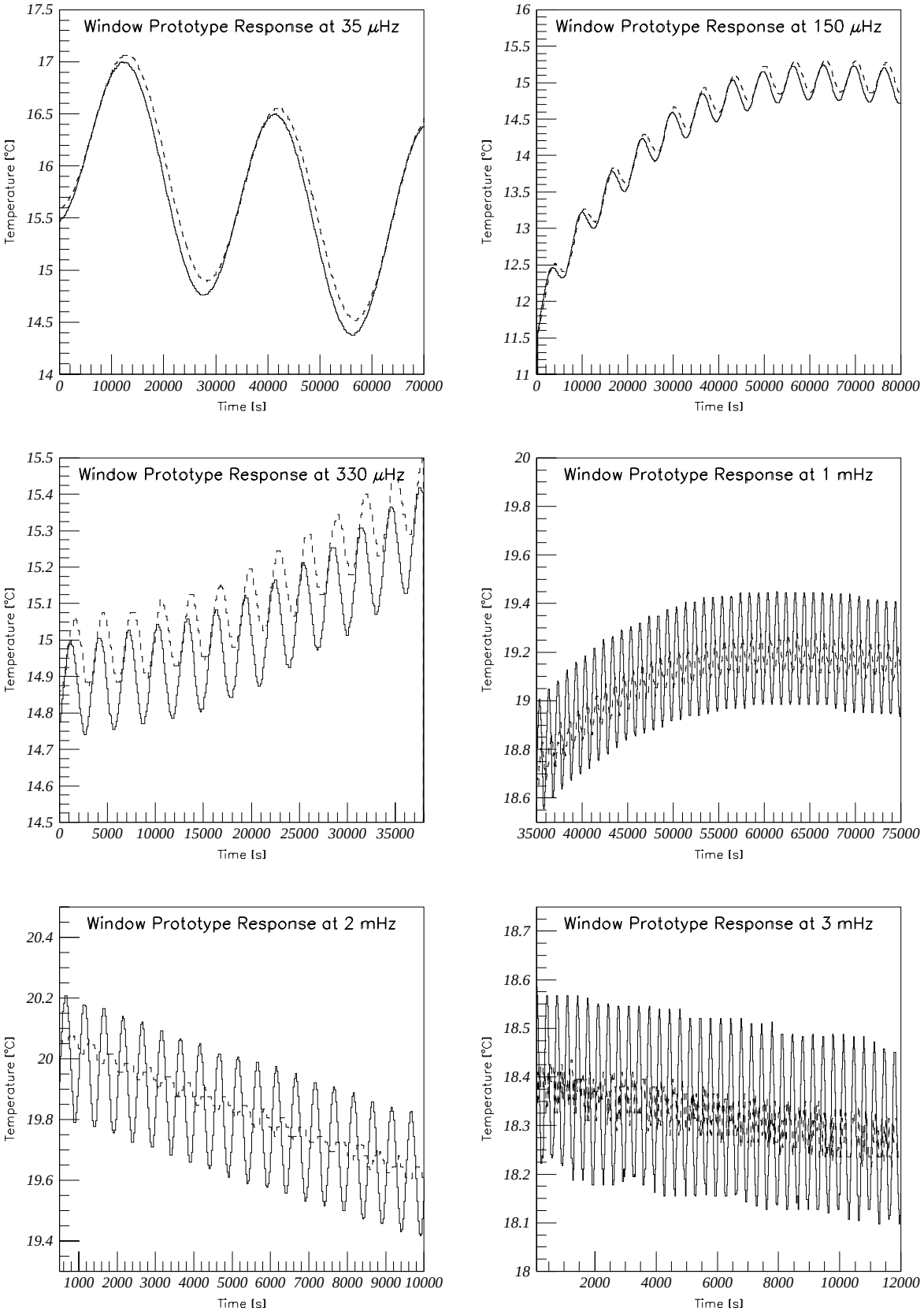

Figure 20: The thermal frequency response of the window prototype

6 Measurements with the feedback loop

The good agreement between the simulated and measured thermal properties of the window in an open loop system lead us to switch on the feed back loop.

The parameters of the controller were set to the values computed in section 2.8:

gain M = 300 W/(m^2 deg)

integrating-to-proportional take-over frequency : $\frac{1}{2\pi\tau_i} = 0.1$ mHz

It should be noted that we do not use any differentiating action.

The set point for the window was 20°C . The temperature of the cooling block was set to 0.5°C. These settings are slightly different than the anticipated settings for the CMS Preshower (18°C and -10°C respectively) but had the advantage of avoiding negative temperatures where ice formation could have jeopardized the internal foam performance (remember that the prototype was not hermetic and therefore its inside volume was not flushed with a neutral gas as will be the case for the Preshower in CMS).

In the first measurement we retained, as for the frequency measurements reported previously, an insulation of the external window. Fig. 21 (bottom) shows the average inside (solid line) and outside (dashed line) temperatures as a function of time for a period of half a day. The inside temperature, used as the input for the regulator, stays constant to within 0.01°C. The outside temperature is also stable to 0.01°C for the first nine hours and then decreases slightly (by about 0.01°C only !) due to a change of the room temperature by ~ -1°C (top of Fig. 21). This shows in fact that the thermal resistance of the external window insulation was rather poor.

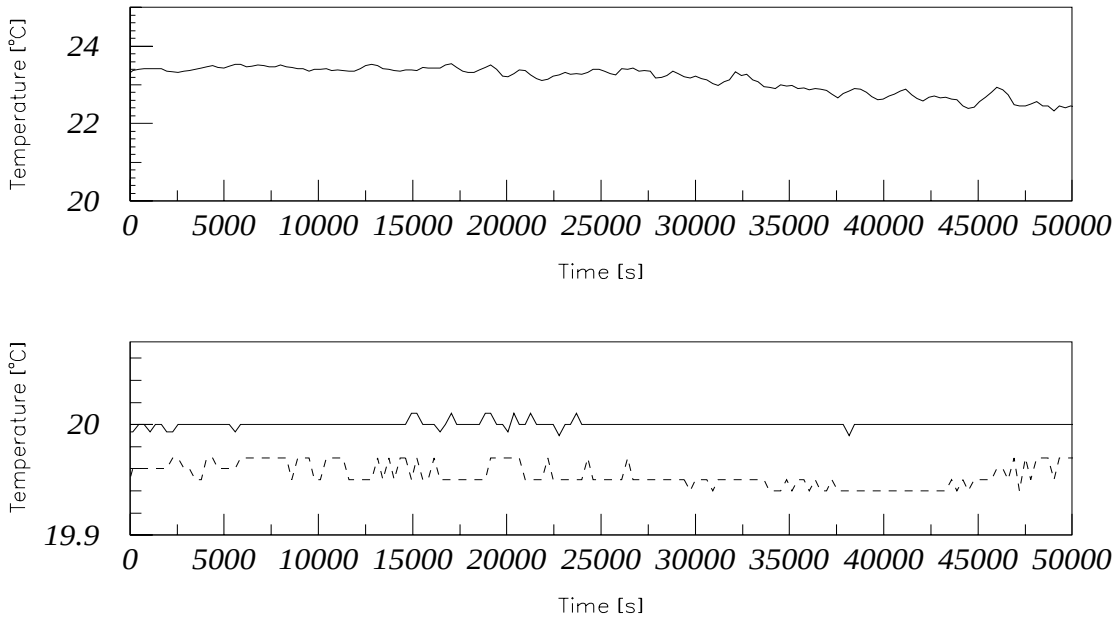

Figure 21: Average inside and outside temperature of the window as a function of time for an insulated setup (bottom). The top plot shows a recording of the room temperature during the same period.

In a second set of measurements, we removed the insulation from the external window face, to be confronted to the worse conditions of external thermal attack. Fig. 22 shows again the room temperature and the average of the window's inside and outside temperatures as a function of time for a period of 2.5 days. A day-night effect of 2°C amplitude is clearly seen on the room temperature. However the (regulated) inside temperature (solid line) is perfectly constant. The outside face temperature is sensitive to the change in the external thermal attack, but the amplitude of the effect is reduced by more than one order of magnitude.

It should be noted that this last measurement corresponds to a very pessimistic case, the external face of the window being subject to unobstructed convection (typically a 15W/m^2 power attack for 1°C difference). In CMS, the very small distance between EE and SE and the cables around EE will reduce drastically the convection possibilities and therefore the sensitivity to changes of the environment temperature.

Note also that the average room temperature was substantially different from the window setpoint: this purely DC

effect is cured by the integrating action of the controller.

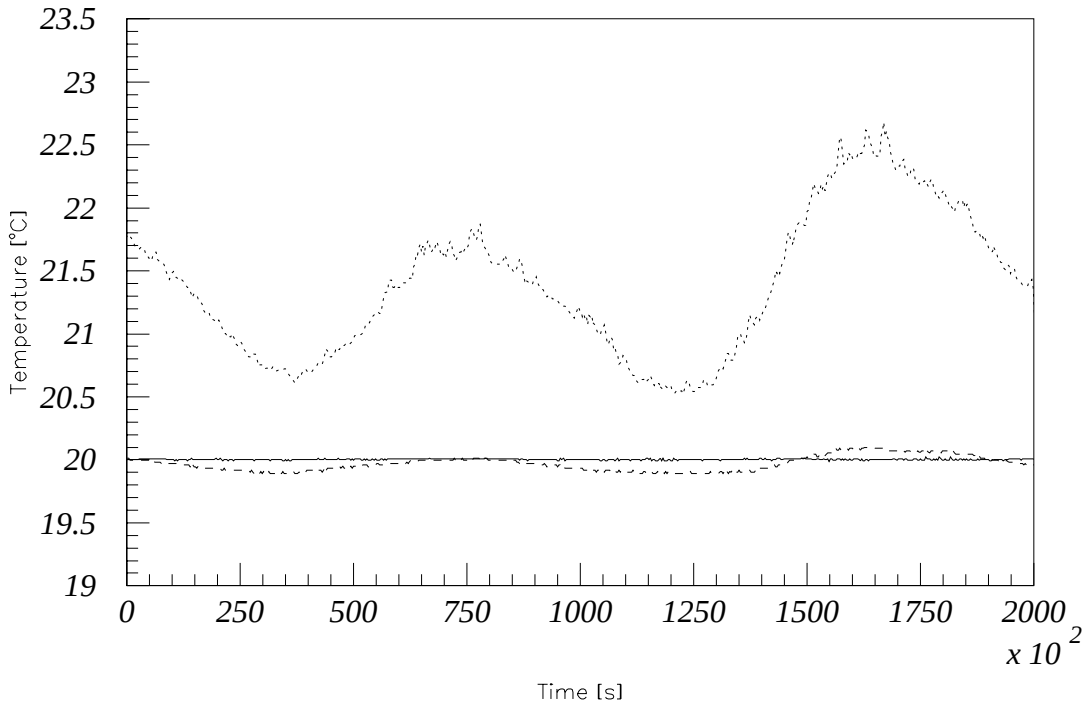

Figure 22: Average window's inside (solid) and outside (dashed) temperature and room temperature (dotted) as a function of time in the case of a non insulated external window's face.

Fig. 23 shows the power delivered by the supply as a function of time during the same 2.5 day test. One sees very nicely the day-night effect on the regulation power which varies to compensate for the change of the external temperature attack.

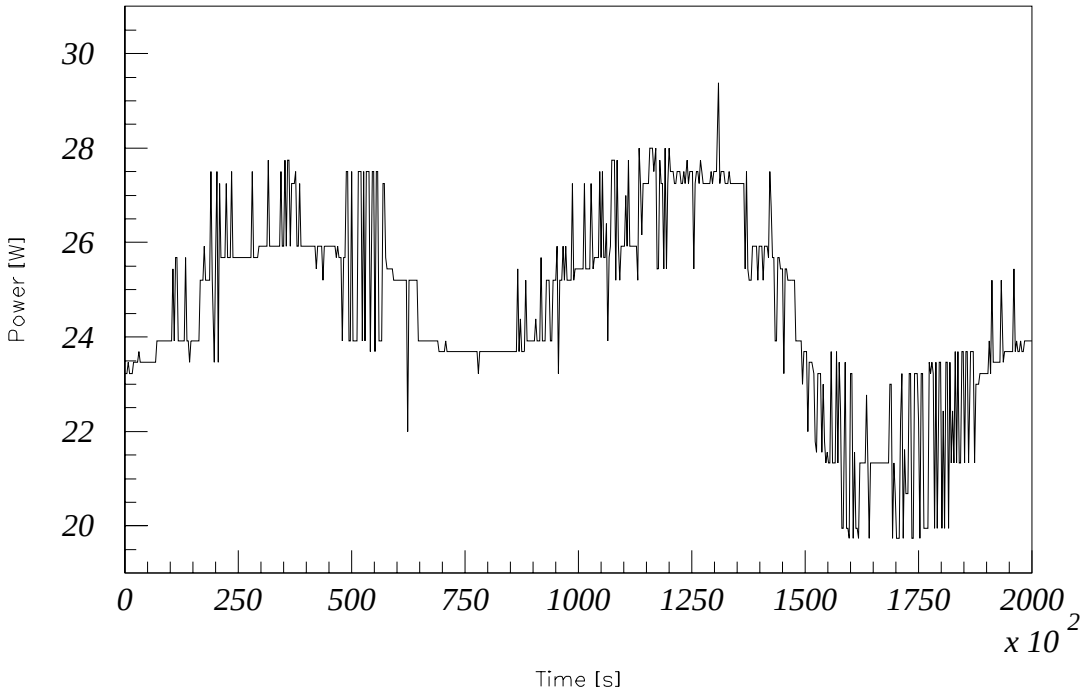

Figure 23: Power supply power as a function of time during the measurement of Fig. 22

To test the robustness of the regulation process, the parameters of the PID were widely varied. When we used the internal temperature readings for feedback, according to our proposal,, we always obtained a very stable behaviour. It is only when using the *external* probes to feedback, increasing the gain M to 800W/(m^2 K) and the integrator's cutoff frequency to 1 mHz, that we could find an unstable (oscillatory) regime, as predicted by the phase behaviour

of the simulations (Fig. 24)

Finally, we studied the effect of a change of the SE internal temperature . The liquid temperature of the cooling system was first increased to 10.5°C . After several hours for stabilization, the liquid temperature was suddenly returned to 0.5 °C to simulate a step change.

Fig. 24 shows the coolant input and output temperatures as a function of time during the last operation. Due to the inertia of the setup, the step stimulus takes in reality about 20 minutes. The behaviour of the inside and outside face temperatures is shown on the bottom of the same figure. The inside face temperature first drops by 0.07°C , then recovers in about 0.7 hours. This is very close to the predicted behaviour , taking into account that the disturbance is 10 times larger than in Fig. 12 and that the step is smeared in time.

The amplitude of the effect on the outside face is more difficult to measure but is again very tiny, as predicted.

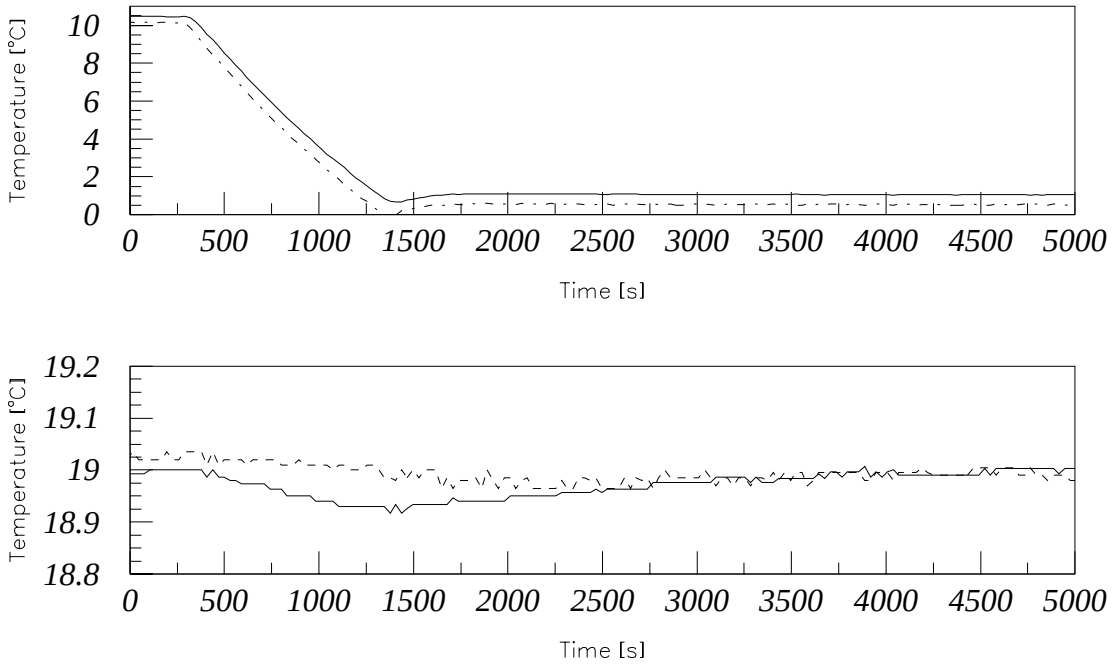

Figure 24: Step change of the SE inside temperature. Top: time dependence of the input and output cooling fluid. Bottom: average inside and outside face temperatures during the same time.Note that for this measurement, the window setpoint was 19°C

7 Conclusions

We have presented a detailed design for the thermal regulation for the Preshower (SE) windows. The windows have, by construction, an inherent suppression of short wavelengths spatial thermal disturbances. This property allows us to propose a simple control layout with a coarse segmentation and without the need for a complicated multivariable controller. Simulations of the windows dynamic response show that a simple closed loop system using a PI controller can provide a stable regime with a very efficient rejection of internal disturbances and an adequate rejection of external disturbances.

This control system has been implemented using industrial hardware and software on a window prototype identical, apart from its lateral dimensions, to the final Preshower window. The measurements are in agreement with the simulations and confirm that a stabilization in time of the SE external face within a few tenths of a degree can be achieved, as requested for the operation of the Endcap Electromagnetic Calorimeter.

References

[1] ECAL Group, *The Electromagnetic Calorimeter Project Technical Design Report*, CERN/LHCC 97-33
[2] Kuo, B. , *Automatic Control Systems* , Prentice-Hall (1991).
[3] The Matlab® software (Matrix Laboratory) by The MathWorks Inc. - see http://www.mathworks.com
[4] Marek ZELANZNY (Eyrolles), *Systemes asservis: commande et regulation*.
[5] J.-ch. GILLE (DUNOD), *Theorie et Calcul des Asservissements lineaires.*
[6] http://www4.ad.siemens.de/, *SIEMENS SIMATIC Modulat PID Control manual*, (ref. C79000-G7076-C121-01)

Annex

List of symbols used in section 2.

s : thickness / Laplace variable = $\sigma+j\omega$

$\omega=2\pi f$: angular freq. in [rad/sec]

f : freq. in [Hz]

sec : second

t : time [sec]

T : temperature (degrees Kelvin AND C)

λ : material thermal conductibility [W/(m K)]

c : material heat capacity [J/(kg K)]

ρ : density [kg/m^3]

j : imaginary unit [-]

v : nodal voltage [V]

i : branch current [W/m^2]

R : specific resistance [K m^2/W]

($1/R$ = conductance per unit panel surface area)

C : capacitance per unit area [J/(m^2 K)]

L : wavelength [m]

$k=2\pi/L$: wave number [m^{-1}]

τ : time constant [sec]

M : regulator gain [W/(m^2 K)]

α : convective heat transfer coefficient

x : state variable